Functionalized Graphene Oxide as a Nanocarrier for Dual Drug Delivery Applications: The Synergistic Effect of Quercetin and Gefitinib Against Ovarian Cancer Cells

9 authors, including:

Himani Tiwari
Kumaun University
12 PUBLICATIONS **198** CITATIONS

SEE PROFILE

Mintu Pal
Nanyang Technological University
39 PUBLICATIONS **1,090** CITATIONS

SEE PROFILE

Souvik Basak
Dr. B. C. Roy College Of Pharmacy and AHS
75 PUBLICATIONS **3,053** CITATIONS

SEE PROFILE

Dr. Ravindra Kumar Verma
Indian Institute of Technology Roorkee
38 PUBLICATIONS **319** CITATIONS

SEE PROFILE

Some of the authors of this publication are also working on these related projects:

PREPARATION OF NANOSTRUCTURED OXIDE MATERIALS AND THEIR CATALYTIC APPLICATIONS IN THE PRODUCTION OF FUELS AND FINE CHEMICALS View project

Isolation of plastic degrading microbe from pharmaceutical waste- a step towards green management of pharmaceutical waste View project

Functionalized graphene oxide as a nanocarrier for dual drug delivery applications: The synergistic effect of quercetin and gefitinib against ovarian cancer cells

Himani Tiwari[a], Neha Karki[a], Mintu Pal[b], Souvik Basak[c], Ravindra Kumar Verma[d], Rajaram Bal[e], Narain Datt Kandpal[f], Ganga Bisht[a], Nanda Gopal Sahoo[a,*]

[a] Nanoscience and Nanotechnology Centre, Department of Chemistry, D.S.B. Campus, Kumaun University, Nainital, Uttarakhand, India
[b] Biotechnology Group, Biological Sciences and Technology Division, CSIR-North East Institute of Science and Technology, Academy of Scientific and Innovative Research, Jorhat, Assam, India
[c] Dr. B.C. Roy College of Pharmacy & Allied Health Sciences, Durgapur 713206, India
[d] National Mission on Himalayan Studies, G.B. Pant National Institute of Himalayan Environment and Sustainable Development, Kosi-Katarmal, Almora, India
[e] Conversion & Catalysis Division, CSIR-Indian Institute of Petroleum, Dehradun, India
[f] Department of Chemistry, S.S.J. Campus, Almora, Kumaun University, Nainital, Uttarakhand, India

ARTICLE INFO

ABSTRACT

Graphene Oxide (GO) has been extensively studied in the field of biomedical sciences as one of the most promising biomaterials due to its exceptional physiochemical properties. Experts have long favored anticancer drug cocktails over single drugs, given that the former may provide a more balanced molecular basis for novel chemotherapeutic strategies. Here, we investigated a combinatorial anticancer drug treatment involving the well-proven anticancer drugs quercetin and gefitinib and compared it with gefitinib and quercetin loaded separately onto polyvinylpyrrolidone (PVP)-functionalized graphene oxide (GO-PVP). The loading and cancer cell cytotoxicity of the individual drug systems and their combined loading onto GO-PVP nanovehicles were investigated in PA-1 ovarian cancer cells and compared to their effects on IOSE-364 ovarian epithelial cells. In this report, the combined drug system loaded on the GO-PVP nanovehicle was found to be significantly more toxic than the individual drug loaded systems, as well as the free drugs, toward PA-1 cells compared to the toxicity toward IOSE-364 cells. The combined drug system loaded on the GO-PVP nanovehicle is likely to be more successful than individual drug therapy, given the stronger impact of the combinatorial approach and the efficiency of chemotherapeutic delivery.

1. Introduction

Nanomaterial-based drug delivery has immense scope in many fields of research; this is particularly true in the field of biomedical sciences because of its value-added properties, such as high loadings, target specificity and controlled or sustained release kinetics in suitable cases [1–8]. Currently, a large number of nanocarriers are being used for the delivery of numerous therapeutic molecules; among these nanocarriers, graphene has become a potential candidate for drug delivery.

Graphene is one-atom thick, comprising 2-D planar sheets. Discovered by Geim et al. in 2004 [9], graphene consists of π-conjugated stratum that may be superficially viewed as a planar aromatic macromolecule. The excellent planar structure of graphene is one of the

main reasons behind its tremendous ability to efficiently capture and embed a large number of substances, including metals, biomolecules, and fluorescent probes [10–14]. Given its excellent ability to easily cross cell membranes and deliver proteins, nucleic acids, and peptides into cells, graphene oxide (GO) can promote the cellular uptake of small drug molecules (e.g., anticancer, antibacterial, or antiviral agents) [15,16] and macromolecules [17,18]. The accessibility of both GO surfaces enables the remarkably high drug loading capacity of GO. In addition, GO presents hydrophilic groups along its edges along with a hydrophobic basal plane. Hence, with its polar groups, GO can extend hydrophilicity to hydrophobic molecules, such as anticancer drugs, which have widely been reported to be loaded onto graphene. Hence, with its excellent properties, such as its small size, high specific surface area (availability of both sides of the sheet), high reactivity, ease of

---

preparation, and superior biocompatibility, the oxidized form of graphene has proven to be a promising candidate for medical and biological applications. Because of these excellent factors, functionalized forms of graphene oxide have been gaining attention as potential carriers in the field of biomedical science. The functionalization of GO with several other molecules can improve its solubility and biocompatibility [19]. Several studies have targeted different molecules for GO functionalization and improved the pharmacokinetics of anticancer drugs. Chitosan [20,21], polyethylene glycol [22], and folic acid [23] are some of the molecules that have been used to functionalize GO. Polyvinylpyrrolidone (PVP) has been used to functionalize grapheme oxide by several authors. Zhi et al. [24] reported the enhanced immunocompatibility of GO when coated with polyvinylpyrrolidone (PVP). As reported by Yang et al. [25], PVP improved the aqueous dispersibility and biocompatibility of reduced grapheme oxide. Swain et al. [26] confirmed that the stability of GO was extended to more than 27 months when coated with PVP-crosslinked polyvinyl alcohol.

Recently, considerable research has been directed toward developing drug delivery systems (DDS), especially for anticancer therapy. Zhang et al. developed a PEG-GO-DOX system for evaluating both *in vitro* and *in vivo* anticancer properties by combining photothermal therapy and chemotherapy in a single system [27]. Hyun Joo Jang et al. reported that the combination of gefitinib and irinotecan could synergistically alleviate colon cancer using a GO-based nanocarrier [28], similar to the HA–GO–DOX nanohybrids [29]. As reported by Yang et al. [25], GO was modified with carboxymethyl chitosan and subsequently conjugated with hyaluronic acid and fluorescein isothiocyanate; onto this conjugate, the anticancer drug doxorubicin was loaded. Highly efficient drug delivery was reported with this system. Wei et al. [30] reported improved cancer therapy using a nanodrug wherein GO was modified with an integrin $\alpha_v\beta_3$ monoclonal antibody (mAb) for tumor targeting. Qin et al. [23] used folic acid conjugated to GO for the chemo-photothermal therapy of cancer.

The first step of the present research was the successful synthesis of graphene oxide using expanded graphite powder as per a modified Hummers method. The aqueous solubility of the as-synthesized GO was due to the presence of highly polar entities, such as hydroxyl, epoxy, and carboxyl groups. This was followed by modification of the GO by grafting it with the highly hydrophilic and biologically compatible polymer, polyvinylpyrrolidone (PVP), to load and deliver the drugs quercetin (QSR) and gefitinib (GEF) together, as well as separately. Here, we report a novel combinatorial drug-conjugation strategy of two drugs, quercetin and gefitinib, two widely used anticancer chemotherapy drugs, with a GO-PVP system. Quercetin and gefitinib are two commonly used anticancer drugs. Gefitinib has shown antitumor activity in nonsmall-cell lung cancer (NSCLC) [31]. It acts by inhibiting signal transmission *via* the epidermal growth factor receptor (EGFR), which is an essential factor for many cell proliferation, growth, and subsequent tissue formation processes [32]. EGFR is basically a tyrosine kinase (TK) subfamily of receptors, and blocking tyrosine kinase is the bottleneck in the strategy of arresting problematic EGFR growth in tumor or metastatic cells [33]. Gefitinib competes with ATP to block the ATP binding domain of TK, thus resulting in dephosphorylation of the enzyme. Following these studies, both individualistic studies [34] and clinical trials [35] have acknowledged the reduction of ovarian tumors by administration of gefitinib. Quercetin has also been reported to have anticancer activity [36,37] in addition to its well-known antioxidant activity. The anticancer activity of quercetin is mainly considered to derive from its inhibitory effect on the cell signaling protein, protein kinase C (PKC-α and PKC-δ). Furthermore, quercetin promotes apoptosis of cancer cells by p53 pathway potentiation, which might be another reason for its cytotoxicity [37]. It may be a plausible assumption that targeting tumors by two different potential pathways will incur a better chance of tumor suppression.

We performed the synthesis, characterization, and subsequent administration of the QSR-GEF drug conjugates. Finally, the release profile of the value-added formulation, together with its concentration-dependent cytotoxicity toward PA-1 ovarian cancer cells using the sulforhodamine B (SRB) assay, were also assessed. The cytotoxic activity of the water-soluble GO-polyvinylpyrrolidone-quercetin-gefitinib (GO-PVP-QSR-GEF) combined complex was significantly higher than that of the GO-polyvinylpyrrolidone quercetin (GO-PVP-QSR) and GO-polyvinylpyrrolidone gefitinib (GO-PVP-GEF) single-drug systems. The resulting combination of the drugs with the nanocarrier (GO-PVP) showed an effective targeting capability and better solubility in biological systems.

2. Materials and methods

2.1. Materials

Expanded graphite powder with a particle size of ˜100 μm was obtained from Sigma-Aldrich, Bangalore, India. Hydrogen peroxide (30% aq.), potassium permanganate, sulfuric acid, and sodium nitrate (NaNO$_3$) were purchased from Himedia; polyvinylpyrrolidone (Mw ˜ 40,000) was purchased from Calbiochem; 4-dimethylaminopyridine (DMAP), and N,N'-dicyclohexylcarbodiimide (DCC) were purchased from SRL, and quercetin (QSR) and gefitinib (GEF) were purchased from Sigma. All other mentioned reagents were purchased from Aldrich and used as received. Eagle's minimum essential medium (MEM) with NEAA, sulforhodamine B assay, penicillin-streptomycin, and fetal bovine serum (FBS) were purchased from Himedia (Assam, India). Unless otherwise indicated, all reagents were acquired from Sigma-Aldrich.

2.2. Sample preparation

Graphene oxide was synthesized in the laboratory from expanded graphite powder by using the traditional Hummers method [38]. The obtained GO was modified with PVP in a carbodiimide-activated esterification reaction [39].

A previously reported method for loading drugs onto GO-PVP was used [39], and 5 mL of a 0.5 mg/mL solution of GO-PVA in deionized water was separately mixed with 0.25 mL of a 8.6 mM solution of QSR in dimethyl sulfoxide (DMSO) and 0.25 mL of a 8.6 mM solution of GEF in DMSO followed by stirring at room temperature for 12 h. Excess amounts of unattached QSR-GEF precipitated as a solid and were removed by centrifuging at 7000 rpm. A 0.8 μm filter was used to fully eliminate any solids from the supernatant, and this solution was dialyzed (molecular weight cut-off MWCO = 3 kDa) with DD water for 2 days to remove the small amount of solubilized free QSR-GEF and DMSO. The obtained GO-PVP-QSR-GEF was stored in the dark sat 5 °C.

2.3. Characterization

The characterization of the synthesized graphene and its related systems, such as GO-PVP and GO-PVP-drugs, was performed with different advanced characteristic techniques.

Thermogravimetric analysis (performed on a TGA 4000, Perkin Elmer) was used for quantitative data acquisition, and the thermal stability of the obtained system was measured at a heating rate of 10 °C/min from 30 °C to 600 °C under a N$_2$ atmosphere (19.2 mL/min). The Fourier transform infrared spectra were recorded on a Perkin Elmer 10.5.2, and Raman spectroscopy (Research India, RIRM-LP1519) was used to study the chemical structures, characteristic changes, and interactions between the drug molecules and the binder. The solubilities of the loaded drugs were observed by UV–vis spectroscopy (Agilent Technologies Cary 60 UV–vis spectrometer). The release behavior of the combined drugs was calculated by absorbance on the UV–vis spectrometer at 374 nm and 331 nm at 35 °C. The surface morphologies of graphene oxide and functionalized GO polymer were analyzed by transmission electron microscopy (TEM). The cellular toxicity and

biocompatibility of combinatorial systems were compared using SRB.

2.4. In vitro combined drug release experiments

The quercetin-gefitinib combination was loaded onto the GO-PVP and evaluated in terms of its stability and release rate with an inner dialysis tube (MWCO = 10 kDa); 2 mL of a prepared GO-PVP-quercetin-gefitinib solution was filled into the dialysis tube and dialyzed with respect to 10 mL of a phosphate buffered saline (PBS) solution (pH 7.4) in an external vial. Afterwards, the closed vial was incubated in a shaker at 35 °C for 72 h. Then, at set time points, 2 mL of the dialysate was removed from the vial and replenished with an equal amount of fresh PBS. The release of the combined drugs from GO-PVP was evaluated by measuring the UV–vis absorbance spectrum at 374 and 331 nm. This experiment was repeated for the single-drug systems loaded onto GO-PVP. The amount of quercetin released from GO-PVP was determined with the help of dissolution studies and evaluated by the UV–vis absorbance spectrum at 374 nm, and that for gefitinib was evaluated at 331 nm.

2.5. Cell culture and in vitro cell viability assay

Ovarian cancer cells (PA-1) were obtained from the National Center for Cell Sciences (NCCS), Pune, India. Nontumorigenic ovarian epithelial cells (IOSE-364) were kind gifts from Dr. Sib Sankar Roy, CSIR-IICB, Kolkata, India. The cells were developed and maintained using an appropriate growth medium, which contained 10% FBS (fetal bovine serum) and 1% penicillin/streptomycin as an antibiotic, in a 5% CO_2 incubator at 37 °C in a humidified atmosphere. A sulforhodamine B assay was performed to determine the relative cell survival percentage after 48 h of treatment, following a previously described method with modifications [40]. In brief, cells (3×10^3/well) were seeded into 96-well plates and exposed to various concentrations (0, 1, 3, 5, and 10 µg/ml) of the synthesized drug-loaded nanocarriers. After 48 h of treatment, 25 µl of cold 50% trichloroacetic acid (TCA) was added to each well, and the plate was kept at 4 °C for 1 h; this was followed by rinsing the wells with water to remove the TCA solution and serum proteins and drying the plates. Next, 50 µl of a 0.4% SRB solution was added to each well and incubated for 30 min, followed by rinsing with 1% acetic acid and air drying. Images were captured using a light microscope. For quantitative measurements, the dye was then solubilized in 100 µl of 10 mM Tris, and the absorbance was spectrophotometrically measured at 565 nm. The cytotoxic effects of the drug-loaded nanocarriers on PA-1 and IOSE-364 cells were determined by the half maximal inhibitory concentration (IC_{50}) in relation to the untreated control, as described earlier [41–44].

3. Result and discussion

3.1. Synthesis, and characterization of GO and functionalized GO

To confirm the successful attachment of the polymer onto the GO sheet, FTIR spectral comparisons between GO and GO-PVP were conducted. The FTIR spectra of GO and grafted GO are shown in Fig. 1. From Fig. 1, as previously reported by our research group for the FTIR spectrum of GO [41], the absorbance peaks at 1048, 1222, 1412, 1635, 1732, and 3435 cm^{-1} can be attributed to alkoxy stretching, epoxy C−O−C, carboxy C−O, C=C skeletal vibrations of graphite domains, carbonyls of −COOH, and hydroxyl groups, respectively (Fig. 1a). After the esterification reaction, the absorbance peak for C=O in GO-PVP had redshifted and become narrower, appearing at 1627 cm^{-1}. Moreover, a sharp doublet peak at 2929 and 2851 cm^{-1} (Fig. 1b) also appeared, which was due to asymmetric and symmetric methylene (−CH$_2$−) stretching. Finally, due to the existence of the polymer (PVP) on the nanocarrier, there were several new peaks after the esterification reaction.
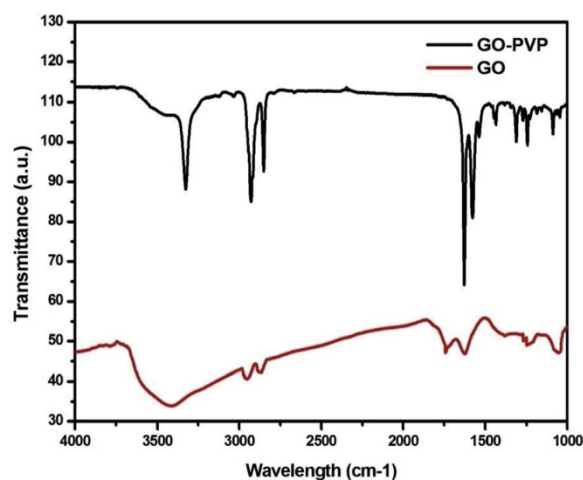

Fig. 1. Fourier-Transform infrared (FT-IR) spectrum of (a) GO, and (b) GO-PVP.
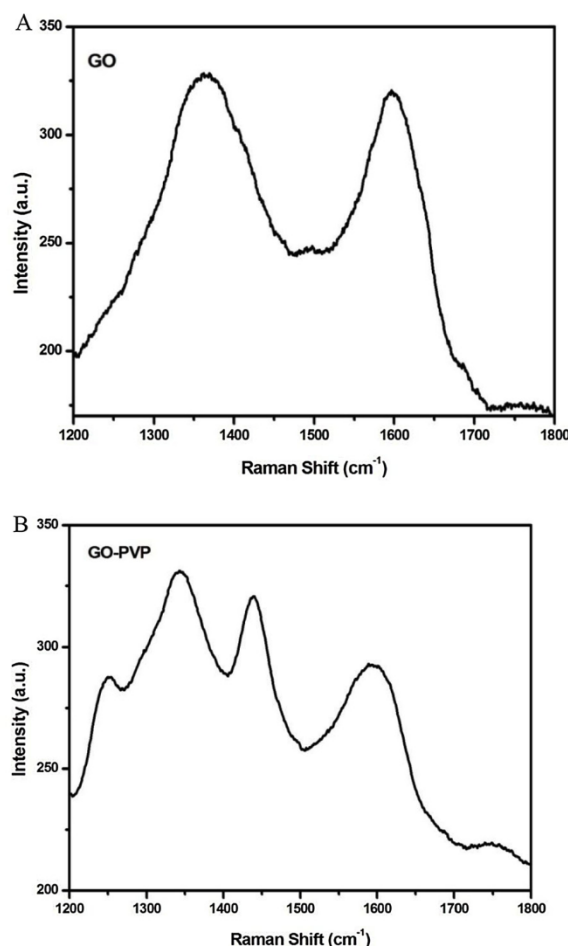

Fig. 2. Raman spectra for (a) GO, and (b) GO-PVP.

The Raman spectra for GO and GO-PVP are shown in Fig. 2. Raman spectra of the pristine graphite, as previously reported, showed a prominent G peak at 1575 cm^{-1} and a weak D peak at 1330 cm^{-1} [45]. In Fig. 2a, the Raman spectra of GO, the G band appeared at 1596 cm^{-1}, and the D band was observed at 1345 cm^{-1}. The G band of GO was due to the C=C double bonds, and the influence of defects as well as the prominent D band indicated a reduction in the amount of in-plane sp^2 domains [46]. In Fig. 2b, the GO-PVP D band was observed at 1343 cm^{-1} and the G band had shifted back to 1588 cm^{-1}, which was
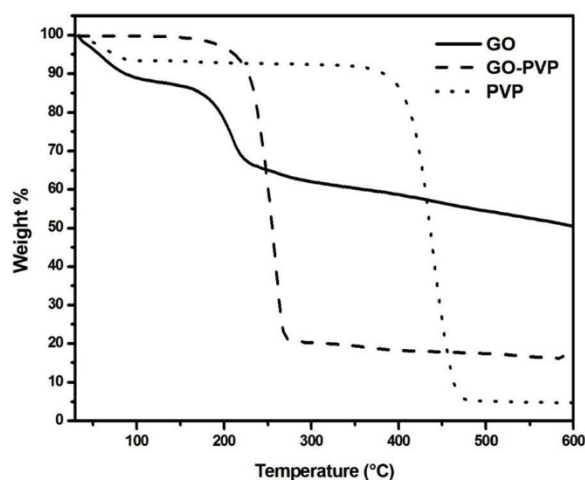
Fig. 3. TGA analysis of GO, GO-PVP, and pure PVP.

somewhat nearer to the G band of the pristine graphite powder than that of GO, signifying that electronic conjugation within the functionalized GO was restored after polymer attachment [47,48]. The ratio of the peak intensities of the characteristic D and G bands shows the degree of disorder on the surface of GO and functionalized GO (GO-PVP). The new peak at 1438 cm^{-1} might be due to the existence of δCH_2 (asym) in the GO-PVP system. As clearly shown in Fig. 2a and b, the ratio of the intensities of the D and G bands (I_D/I_G) for GO was 1.005, while the I_D/I_G ratio for GO-PVP was 1.129. This increase in the intensity ratio from 1.005 to 1.129 was due to the sp^2 hybridized carbon atoms, which changed to sp^3 hybridized carbon atoms on the GO surface after functionalization with PVP. This indicated the successful adsorption of PVP onto the basal plane of GO, reflecting the more chaotic structure of GO-PVP [41].

The thermal analysis of the materials was analyzed by using TGA, in which changes in the chemical and physical properties of the materials were measured with respect to temperature (constant heating rate) or time (constant temperature and/or constant mass loss) [49]. Fig. 3 shows the overall quantitative results for PVP grafted onto the graphene oxide sheets. From the TGA spectra, it can be clearly observed that the thermal stability of graphene oxide was not good, and because of the volatilization of stored H$_2$O in the π-stacked structure of GO, mass loss started below 100 °C [50]. The first major, rapid mass loss was observed at approximately 190 °C, which was due to the pyrolysis of the oxygenated groups of GO [46]. The thermal stability of the GO sheets increased upon functionalization of GO with PVP. At a temperature of 600 °C under an inert nitrogen atmosphere, the TGA data showed an 84% mass loss for GO-PVP, whereas pure PVP and GO showed mass losses of 95% and 48%, respectively. Here, the TGA thermograms also indicated that the interaction between GO and the PVP polymer improved the thermal stability. Therefore, it could be concluded that the PVP-grafted graphene oxide consisted of approximately 23 wt% GO and 77 wt% PVP.

In addition, the morphologies of the modified GO and functionalized GO were investigated by TEM, and the results are shown in Fig. 4. The endogenous wrinkled lamellar morphology of the GO sheet can clearly be seen in Fig. 4a, which reflected the successful synthesis of GO from the powdered expanded graphite by using the modified Hummers method. Fig. 4b clearly displays a homogeneous and smooth morphology for PVP on the underlying structure of GO, causing no distortions. It is also clear from Fig. 4b that the surface of polymer-functionalized GO was thicker than that of graphene oxide alone, and the wrinkled sheet of GO was clearly converted into a smooth patch-like layered structure in the GO-PVP composite. The material depicted in Fig. 4b has darker patches on the GO sheet, which resulted from the functionalization procedure.

The colloidal size distribution of GO–PVP in an aqueous solution was characterized by dynamic light scattering (DLS), and the results are shown in Fig. 5. The hydrodynamic particle size distribution graph suggested that there was biomodal distribution of nanoparticles. The peak of the size distribution curve for GO-PVP was centered at approximately 300–400 nm, which was greater than the previously reported average size (166.5 nm) of GO [45]. It was also observed that the zeta potential of the nanoparticles is ˜ − 50 mV which indicated that stable particles in the solution or suspension. The increase in the average size should result from the PVP grafted onto the graphene sheets.

3.2. Evaluation of drug loading, release profile and in vitro cytotoxicity of the dual drug nanoconjugate

3.2.1. UV–vis spectroscopy

To study the combined drug loading of quercetin (QSR) and gefitinib (GEF) onto the nanocarrier delivery system, UV–vis spectroscopy was used. The analysis was performed in a laboratory environment over a range of 200–800 nm (λ). According to our strategy, first QSR was loaded onto GO-PVP by the addition of a solution of QSR in DMSO to the nanocarrier; subsequently, GEF was added with continuous stirring. By repeated ultrafiltration and centrifugation, the unattached and undissolved drugs were removed, and the GO-PVP-QSR-GEF composite was obtained. To characterize the loading capacity of the combinatorial drug onto the GO-PVP system, we first studied the UV–vis spectra of GO and GO-PVP (Fig. 6a). A band appeared at 225 nm corresponding to the π-to-π* transitions of the aromatic carbon-carbon double bond (C=C) in graphene oxide, while in GO-PVP, a new peak was observed at ˜275 nm; the peak at 225 nm, which was present in the spectra of GO, disappeared. This confirmed the grafting of PVP onto GO and the presence of PVP in the prepared composite. By using the Beer-Lambert law (A = €Cx, where A is the absorbance, € is the molar extinction coefficient, which is 0.0031 × 10^6 M^{-1} cm^{-1} for gefitinib and 6.3197 × 10^2 M^{-1} cm^{-1} for quercetin, C is the concentration of the drug sample, and x is the thickness of the cuvette, 1 cm), the drug loading onto the functionalized GO at different concentrations was evaluated. It was estimated that 20% of GEF was loaded onto the GO-PVP-GEF composite and 14% of QSR was loaded onto the GO-PVP-QSR system; in the GO-PVP-QSR-GEF dual drug delivery system, 20% of QSR and 46% of GEF were loaded onto the GO-PVP nanocarrier. Fig. 6b shows the UV–vis spectra of QSR loaded onto the GO-PVP nanocarrier system at three different concentrations. In Fig. 6b, a sharp peak is clearly visible at ˜380 nm, which indicated the presence of quercetin. The peak in the range of 330–340 nm in Fig. 6c indicates the presence of gefitinib in the GO-PVP system at three different concentrations in which a sharp peak was displayed for the initial concentration of the drug with the binder. The UV–vis spectrum of the dual drug-loaded system was recorded, in which a peak appeared at ˜380 nm corresponding to quercetin and a very small peak appeared at ˜331 nm for gefitinib (Fig. 6d). This clearly indicated that both QSR and GEF were successfully loaded onto the GO-PVP nanocarrier.

3.2.2. Release performance of combined drugs

To determine the solubility of the combined loading of QSR and GEF onto GO-PVP, the release behavior of the combinatorial system was analyzed. Fig. 7 shows the in vitro release performance of the combined drugs from the GO-PVP system in PBS at pH 7.4 and 35 °C over 72 h. Previous reports have indicated that the in vitro release profiles of most anticancer drugs from functionalized GO varies slowly in aqueous medium at pH 7 [26]; this slow release is considered to be due to hydrophobic interactions and H-bonding between the drugs and GO sheets. Here, we report the release profile diagram in a buffer solution at pH 7.4. It is clearly seen in Fig. 7b that the release rate of the combinatorial drug from the GO-PVP nanocarrier in a fresh PBS solution was better than the release behavior of the individual drugs from
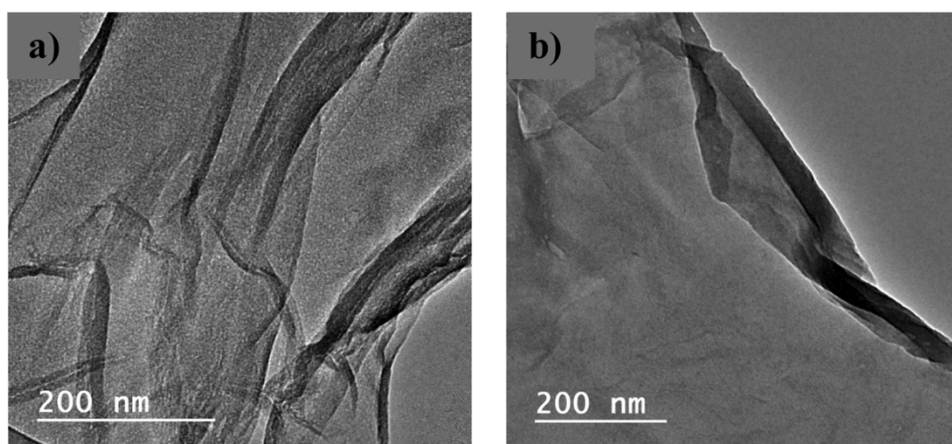
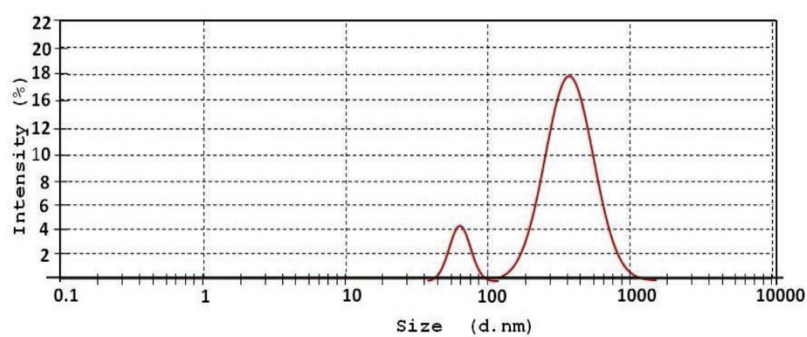**Fig. 4.** TEM photographs of (a) GO, and (b) GO-PVP.
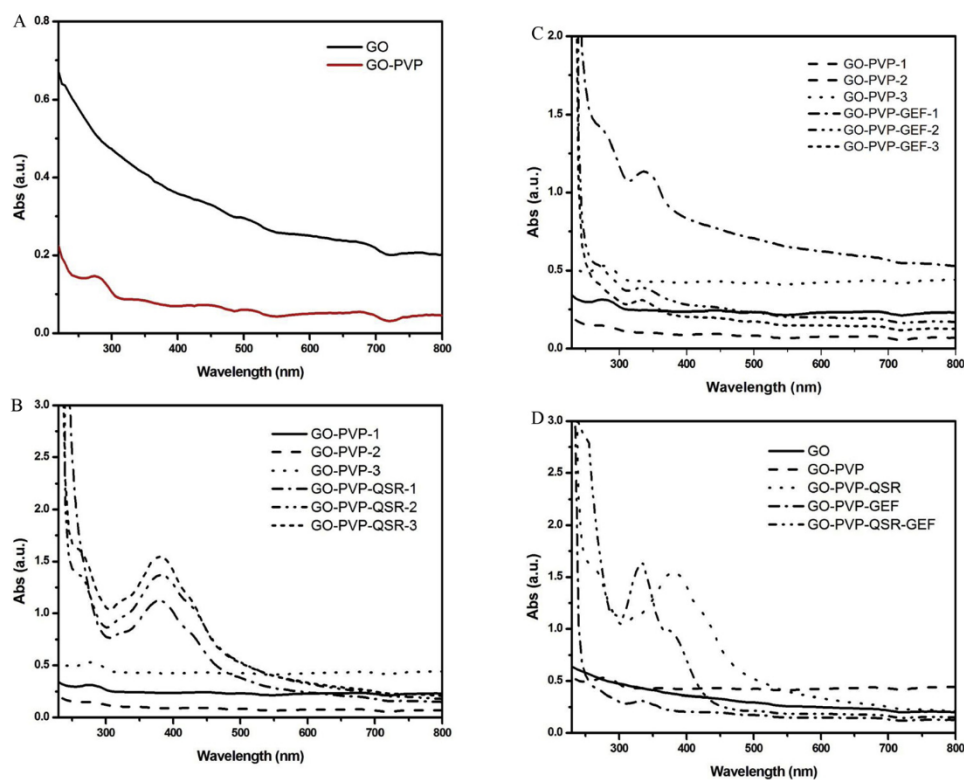

Fig. 5. DLS image of GO-PVP.

Fig. 6. UV–vis absorption spectrum of (a) GO/GO-PVP, and (b) GO-PVP/GO-PVP-QSR (c) GO-PVP /GO-PVP-GEF, and (d) GO/GO-PVP/GO-PVP-QSR/GO-PVP–GEF /GO-PVP-QSR-GEF.
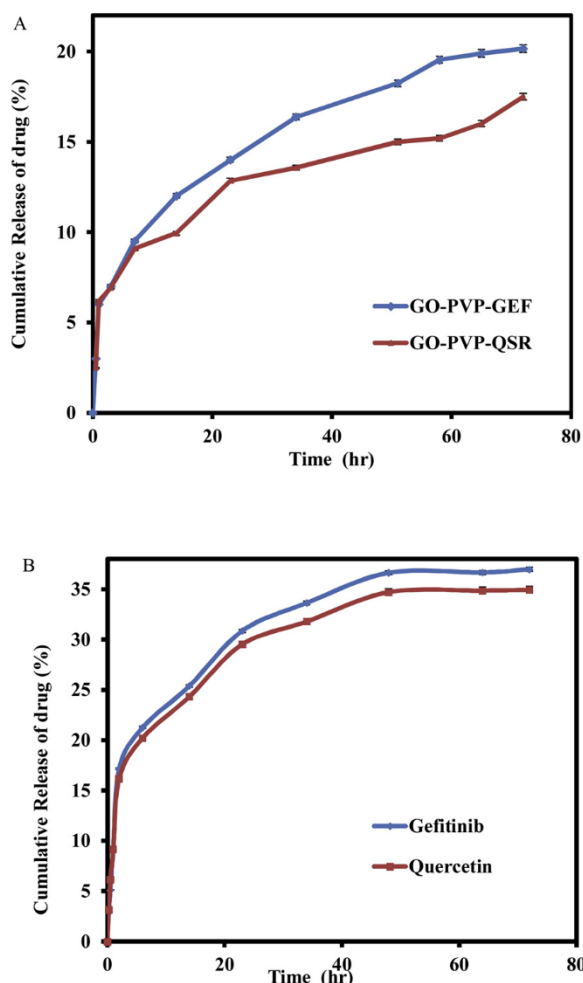
Fig. 7. Drug release at pH 7.4 of (a) GO-PVP-QSR, and GO-PVP-GEF, and (b) combinatorial release of GO-PVP-QSR-GEF at pH 7.4 in PBS at 35 °C. All data are presented as mean ± SD (n = 8).

Fig. 8. (a) Cell viability of IOSE normal Ovarian cells with different concentrations of GO- PVP/GO-PVP-QSR/GO-PVP-GEF/GO-PVP-QSR-GEF, and QSR-DMSO/GEF-DMSO, and (b) Cell viability of PA-1 Ovarian cancer cells with different concentrations of GO- PVP/GO-PVP-QSR/GO-PVP-GEF/GO-PVP-QSR-GEF, and QSR-DMSO/GEF-DMSO. All data are presented as mean ± SD (n = 3).

the same nanocarrier (Fig. 7a). It could be concluded that in the case of each of the two drugs, when loaded individually, the release profile at pH 7.4 over 72 h in PBS was quite poor and found to only be approximately 20% of the total loaded GEF and approximately 18% of total loaded QSR on the surface of the polymer-functionalized GO. This may be understood with the help of intermolecular interactions, such as π-π stacking between the aromatic drug molecules and the carrier. Both drug molecules have a high abundance of electronegative atoms, such as fluorine, chlorine, nitrogen, and oxygen, which may result in strong inter- and intramolecular H-bonding. It was observed that 34–37% of the total combined drug loading on the GO nanocarrier was released within 72 h at 35 °C. Clearly, GO-PVP was an excellent high-efficacy drug delivery system, delivering not one but two drugs simultaneously. Because of the improved drug loading and releasing abilities of polymer-grafted graphene oxide toward the combined drugs, it was proven that this system is an excellent nanovehicle not only for single-drug loading but also for combined drug delivery systems [21].

3.2.3. Cellular uptake and in vitro cytotoxicity experiment of the combined drug loaded nanovehicle

In vitro cytotoxicity of the combined drugs loaded onto the nanocarrier was performed by an SRB assay using GO-PVP in PA-1 and IOSE-364 cells. At a concentration of 10 mg/L, the viability of the IOSE normal ovarian cells remained at approximately 83%, 86%, 76%, and 83% for the GO-PVP, GO-PVP-QSR, GO-PVP-GEF, and GO-PVP-QSR-GEF systems, respectively, indicating no significant cytotoxic effects on
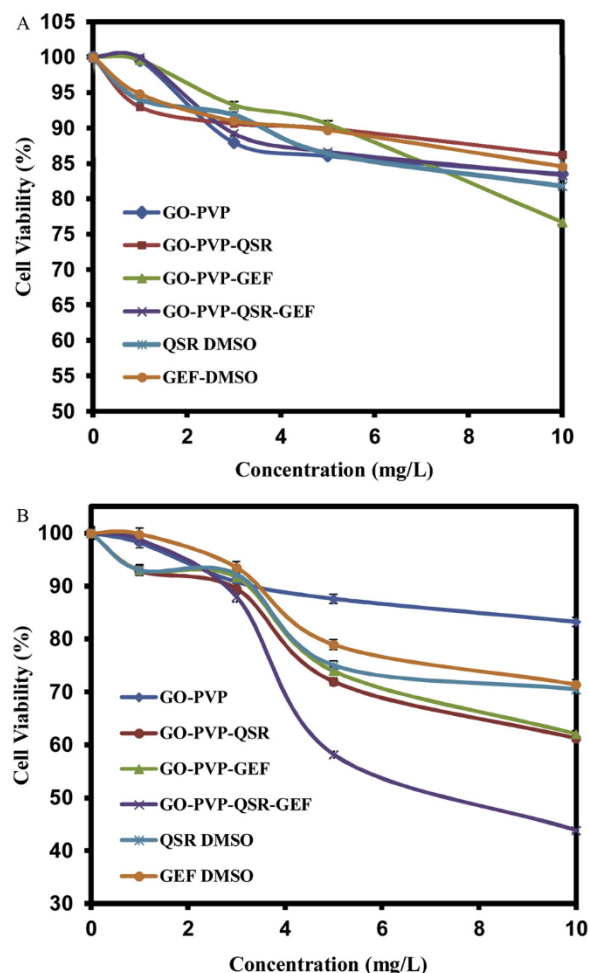
the IOSE cells (Fig. 8a). Furthermore, the comparative chemotherapeutic activity, *i.e.*, percentage of cell growth inhibition of PA-1 ovarian cancer cells, of GO-PVP, GO-PVP-GEF, GO-PVP-QSR, the combinatorial system, and the pure drugs alone is shown in Fig. 8b. The viabilities of the PA-1 ovarian cancer cells were 83%, 61%, 62%, and 43% for GO-PVP, GO-PVP-QSR, GO-PVP-GEF, and GO-PVP-QSR-GEF, respectively, at a concentration of 10 mg/L. GO-PVP-QSR-GEF showed a half maximal inhibitory concentration in PA-1 ovarian cancer cells of 97 µM, whereas those of GO-PVP-QSR, GO-PVP-GEF, and the pure drugs in DMSO were 288 µM, 210 µM, and 237 µM, respectively, suggesting that GO-PVP-QSR-GEF had a significant cytotoxicity (p < 0.5), in comparison to that of the single-drug systems as well as the pure drugs, toward PA-1 ovarian cancer cells at the aforementioned concentrations after 48 h of treatment. However, to investigate the non-specific cytotoxicity of the combined drugs loaded onto the GO-PVP nanocarrier, cellular morphological images were taken of normal ovarian cancer cells incubated with the maximal therapeutic concentration of GO-PVP-QSR-GEF determined in our study (Fig. 9a and b).

As shown in Fig. 8, cytotoxic effects for the combined drugs at a concentration as high as 10 µg/mL were not observed for PA-1 normal ovarian cells. Thus, overall, it can be suggested that GO-PVP-QSR-GEF can be a potential nanodrug conjugate for improved delivery and enhanced cellular uptake without considerable cytotoxicity toward selected cancer cells.
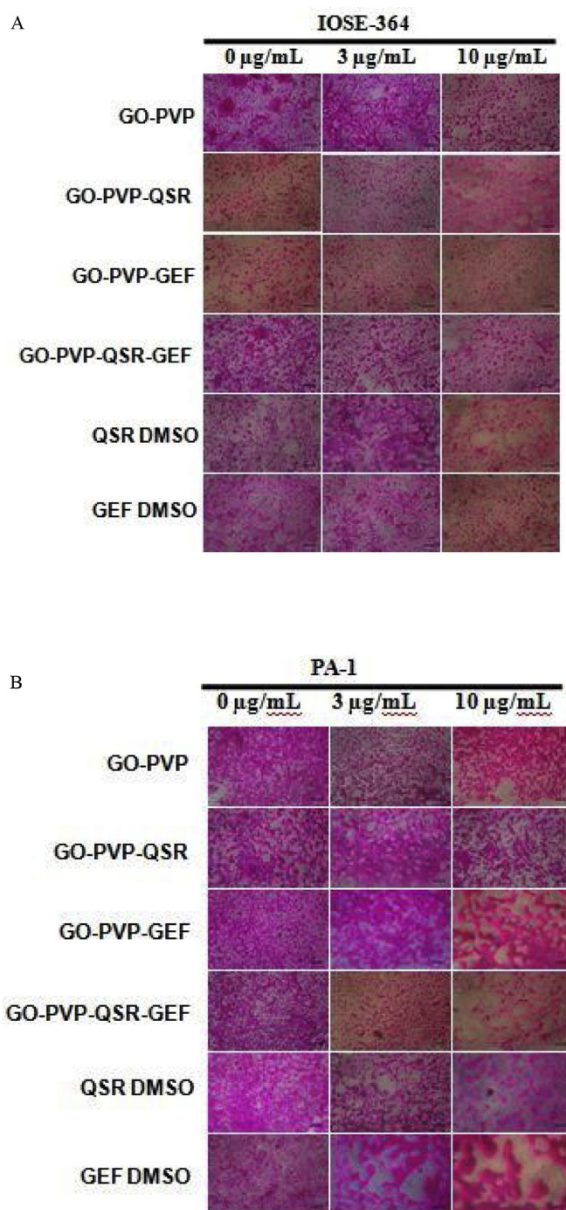
Fig. 9. Phase contrast microscopic images showing the morphological changes of (A) IOSE-364, and (B) PA-1 cells after treatment with indicated drug-loaded nanocarriers at 48 h treatment at 0,1, 3, 5, and 10 ug/ml concentrations.

4. Conclusion

In summary, we have reported the synthesis of GO and PVP-grafted GO as a nanocarrier with acceptable biocompatibility, efficient loading, improved drug release, and enhanced anticancer activity within a certain dose range. This study has demonstrated that the functionalization of GO with polymers such as PVP considerably enhances its solubility and biocompatibility. The chemical structure and morphology of the synthesized GO-PVP were characterized by Raman spectroscopy, TGA analysis, and FTIR spectroscopy. The efficient and targeted delivery of combinatorial anticancer drugs loaded onto GO-PVP into cells *via* receptor-mediated endocytosis was established through cellular uptake experiments and cytotoxicity tests. Furthermore, two anticancer drugs, quercetin, and gefitinib, were loaded together onto GO-PVP, exhibiting higher cytotoxicity to PA-1 ovarian cancer cells in comparison to the individual drugs loaded onto the GO polymer composite. To the best of our knowledge, this is the first attempt to load a binary drug conjugate onto a single nanocarrier to target a specific disease with considerable

therapeutic efficiency and low cytotoxicity.

References

[1] K.N. Burger, R.W. Staffhorst, H.C. de Vijlder, M.J. Velinova, P.H. Bomans, P.M. Frederik, B. de Kruijff, Nanocapsules: lipid-coated aggregates of cisplatin with high cytotoxicity, Nat. Med. 8 (2002) 81–84.
[2] W. Wei, G. Ma, G. Hu, D. Yu, T. McLeish, Z. Su, Z. Shen, Preparation of hierarchical hollow CaCO$_3$ particles and the application as anticancer drug carrier, J. Am. Chem. Soc. 130 (2008) 15808–15810.
[3] L. Tang, Y. Wang, Y. Li, J. Du, J. Wang, Shell-detachable micelles based on disulfide-linked block copolymer as potential carrier for intracellular drug delivery, Bioconjugate Chem. 20 (2009) 1095–1099.
[4] Z. Liu, X. Sun, N. Nakayama-Ratchford, H. Dai, Supramolecular chemistry on watersoluble carbon nanotubes for drug loading and delivery, ACS Nano 1 (2007) 50–56.
[5] S. Santra, C. Kaittanis, J. Grimm, J.M. Perez, Drug/dye-loaded, multifunctional iron oxide nanoparticles for combined targeted cancer therapy and dual optical/magnetic resonance imaging, Small 5 (2009) 1862–1868.
[6] R. Guo, R. Li, X. Li, L. Zhang, X. Jiang, B. Liu, Dual-functional alginic acid hybrid nanospheres for cell imaging and drug delivery, Small 5 (2009) 709–717.
[7] S. Purushotham, R.V. Ramanujan, Thermoresponsive magnetic composite nanomaterials for multimodal cancer therapy, Acta Biomater. 6 (2010) 502–510.
[8] M. Yokoyama, S. Fukushima, R. Uehara, K. Okamoto, K. Kataoka, Y. Sakurai, T. Okano, Characterization of physical entrapment and chemical conjugation of adriamycin in polymeric micelles and their design for in vivo delivery to a solid tumor, J. Control. Release 50 (1998) 79–92.
[9] K.S. Novoselov, A.K. Geim, S.V. Morozov, D. Jiang, Y. Zhang, S.V. Dubonos, I.V. Grigorieva, A.A. Firsov, Electric field effect in atomically thin carbon films, Science 302 (2004) 666–669.
[10] Y. Wang, Z. Li, J. Wang, J. Li, Y. Lin, Graphene and graphene oxide: biofunctionalization and applications in biotechnology, Trends Biotechnol. 29 (2011) 205–212.
[11] L. Feng, L. Wu, X. Qu, New horizons for diagnostics and therapeutic applications of graphene and graphene oxide, Adv. Mater. 25 (2013) 168–186.
[12] G. Gonçalves, M. Vila, M.T. Portolés, M. Vallet-Regi, J. Gracio, P.A.A.P. Marque, Nano-graphene oxide: a potential multifunctional platform for cancer therapy, Adv. Healthcare Mater. (2013) 1–19.
[13] K. Yang, L. Feng, X. Shi, Z. Liu, Nano-graphene in biomedicine: theranostic applications, Chem. Soc. Rev. 42 (2013) 530–547.
[14] L. Feng, Z. Li, Graphene in biomedicine: opportunities and challenges, Nanomedicine 6 (2011) 317–324.
[15] X. Sun, Z. Liu, K. Welsher, J.T. Robinson, A. Goodwin, S. Zaric, H. Dai, Nano-graphene oxide for cellular imaging and drug delivery, Nano Res. 1 (2008) 203–212.
[16] Z. Liu, J.T. Robinson, X. Sun, H. Dai, Pegylated nanographene oxide for delivery of water-insoluble cancer drugs, J. Am. Chem. Soc. 130 (2008) 10876–10877.
[17] Y. Wang, Z. Li, D. Hu, C.T. Lin, J. Li, Y. Lin, Aptamer/graphene oxide nanocomplex for in situ molecular probing in living cells, J. Am. Chem. Soc. 132 (2010) 9274–9276.
[18] C.H. Lu, C.L. Zhu, J. Li, J.J. Liu, X. Chen, H.H. Yang, Using graphene to protect DNA from cleavage during cellular delivery, Chem. Commun. 46 (2010) 3116–3118.
[19] Y. Wang, Z. Li, J. Wang, J. Li, Y. Lin, Graphene and graphene oxide: biofunctionalization and applications in biotechnology, Trends Biotechnol. 29 (2011) 205–212.
[20] A. Deb, R. Vimala, Natural and synthetic polymer for graphene oxide mediated anticancer drug delivery–a comparative study, Int. J. Biol. Macromol. 107 (2018) 2320–2333.
[21] H. Bao, Y. Pan, Y. Ping, N.G. Sahoo, T. Wu, L. Li, J. Li, L.H. Gan, Chitosan-functionalized graphene oxide as a nanocarrier for drug and gene delivery, Small 7 (2011) 1569–1578.
[22] Z. Xu, S. Wang, Y. Li, M. Wang, P. Shi, X. Huang, Covalent functionalization of graphene oxide with biocompatible poly(ethylene glycol) for delivery of paclitaxel, ACS Appl. Mater. Interfaces 6 (2014) 17268–17276.
[23] X.C. Qin, Z.Y. Guo, Z.M. Liu, W. Zhang, M.M. Wan, B.W. Yang, Folic acid-conjugated graphene oxide for cancer targeted chemo-photothermal therapy, J. Photobiol. B: Biol. 120 (2013) 156–162.
[24] X. Zhi, H. Fang, C. Bao, G. Shen, J. Zhang, K. Wang, S. Guo, T. Wan, D. Cui, The immunotoxicity of graphene oxides and the effect of PVP-coating, Biomaterials 34 (2013) 5254–5261.
[25] H. Yang, D.H. Bremner, L. Tao, H. Li, J. Hu, L. Zhu, Carboxymethyl chitosan-mediated synthesis of hyaluronic acid-targeted graphene oxide for cancer drug delivery, Carbohyd. Polym. 135 (2016) 72–78.
[26] A.K. Swain, D. Bahadur, Enhanced stability of reduced graphene oxide colloid using cross- linking polymers, J. Phys. Chem. C 118 (2014) 9450–9457.
[27] W. Zhang, Z.Y. Guo, D.Q. Huang, Synergistic effect of chemo-photothermal therapy using pegylated graphene oxide, Biomaterials 32 (2011) 8555–8561.
[28] H.J. Jang, E.M. Hong, J. Jang, J.E. Choi, S.W. Park, H.W. Byun, D.H. Koh,

M.H. Choi, S.H. Kae, J. Lee, Synergistic effects of simvastatin and irinotecan against colon cancer cells with or without irinotecan resistance, Gastroenterol. Res. Pract. (2016) 1–9.

[29] E. Song, W. Han, C. Li, D. Cheng, L. Li, L. Liu, G. Zhu, Y. Song, W. Tan, Hyaluronic acid-decorated graphene oxide nanohybrids as nanocarriers for targeted and ph-responsive anticancer drug delivery, ACS Appl. Mater. Interfaces 6 (2014) 11882–11890.

[30] Y. Wei, F. Zhou, D. Zhang, Q. Chen, D. Xing, A graphene oxide based smart drug delivery system for tumor mitochondria-targeting photodynamic therapy, Nanoscale 8 (2016) 3530–3538.

[31] T.J. Lynch, A.A. Adjei, P.A. Bunn, T.G. Eisen, J. Engelman, G.D. Goss, D.A. Haber, J.V. Heymach, P.A. Janne, B.E. Johnson, D.H. Johnson, R.C. Lilenbaum, M. Meyerson, A.B. Sandler, L.V. Sequist, J. Settleman, K.K. Wong, C.S. Hart, Summary statement: novel agents in the treatment of lung cancer: advances in epidermal growth factor receptor-targeted agents, Clin. Cancer Res. 12 (2006) 4365–4371.

[32] S. Basak, S. Mondal, S. Dey, P. Bhattacharya, A. Saha, V.D. Punetha, A. Abbas, N.G. Sahoo, Fabrication of β-cyclodextrin-mediated single bimolecular inclusion complex: characterization, molecular docking, in-vitro release and bioavailability studies for gefitinib and simvastatin conjugate, J. Pharm. Pharmacol. 69 (2017) 1304–1317.

[33] M. Gupta, K. Goswami, R.K. Marwaha, H. Dureja, Safety and antitumor activity of gefitinib: an overview, Int. J. Pharm. Sci. Res. 5 (2014) 4129–4140.

[34] W. Wen, J. Wu, L. Liu, Y. Tian, R. Buettne, M.Y. Hsieh, D. Horne, T.H. Dellinger, E.S. Han, R. Jove, J.H. Yim, Synergistic anti-tumor effect of combined inhibition of EGFR and JAK/STAT3 pathways in human ovarian cancer, Mol. Cancer 14 (2015) 1–11.

[35] E.M. Posadas, M.S. Liel, V. Kwitkowski, L. Minasian, A.K. Godwin, M.M. Hussain, V. Espina, B.J. Wood, S.M. Steinberg, E.C. Kohn, A phase II and pharmacodynamic study of gefitinib in patients with refractory or recurrent epithelial ovarian cancer, Cancer 109 (2007) 1323–1330.

[36] A. Parvaresh, R. Razavi, N. Rafie, R. Ghiasvand, M. Pourmasoumi, M. Miraghajani, Quercetin and ovarian cancer: an evaluation based on a systematic review, J. Res. Med. Sci. 21 (2016) 34–40.

[37] M. Hashemzaei, A.D. Far, A. Yari, R.E. Heravi, K. Tabrizian, S.M. Taghdisi, S.E. Sadegh, K. Tsarouhas, D. Kouretas, G. Tzanakakis, D. Nikitovic, N.Y. Anisimov, D.A. Spandidos, A.M. Tsatsakis, R. Rezaee, Anticancer and apoptosis inducing effects of quercetin in vitro and in vivo, Oncol. Rep. 38 (2017) 819–828.

[38] W.S. Hummers, R.E. Offeman, Preparation of graphitic oxide, J. Am. Chem. Soc. 80 (1958) 1339.

[39] N.G. Sahoo, H. Bao, Y. Pan, M. Pal, M. Kakran, H. Kuo, F. Cheng, L. Lia, L.P. Tan, Functionalized carbon nanomaterials as nanocarriers for loading and delivery of poorly water soluble anticancer drug: a comparative study, Chem. Commun. 47 (2011) 5235–5237.

[40] V. Vichai, K. Kirtikara, Sulforhodamine B colorimetric assay for cytotoxicity screening, Nat. Protoc. 1 (2006) 1112–1116.

[41] N. Karki, H. Tiwari, M. Pal, A. Chaurasia, R. Bal, P. Joshi, N.G. Sahoo, Functionalized graphene oxides for drug loading, release and delivery of poorly water soluble anticancer drug: a comparative study, Colloids Surf. B 169 (2018) 265–272.

[42] I. Saikia, S. Sonowal, M. Pal, P.K. Boruah, M.R. Das, C. Tamuly, Biosynthesis of gold decorated reduced graphene oxide and its biological activities, Mater. Lett. 178 (2016) 239–242.

[43] I. Saikia, M. Hazarika, S. Yunus, M. Pal, M.R. Das, J.C. Borah, C. Tamuly, Green synthesis of Au-Ag-In-rGO nanocomposites and its α-glucosidase inhibition and cytotoxicity effects, Mater. Lett. 211 (2018) 48–50.

[44] N.B. Allou, A. Yadav, M. Pal, R.L. Goswamee, Biocompatible nanocomposite of carboxymethyl cellulose and functionalized carbon–norfloxacin intercalated layered double hydroxides, Carbohydr. Polym. 186 (2018) 282–289.

[45] Y. Pan, H. Bao, N.G. Sahoo, T. Wu, Lin Li, Water-soluble poly (n -iso-propylacrylamide)–graphene sheets synthesized via click chemistry for drug delivery, Adv. Funct. Mater. 21 (2011) 2754–2763.

[46] S. Stankovich, D.A. Dikin, R.D. Piner, K.A. Kohlhaas, A. Kleinhammes, Y. Jia, Y. Wu, S.B.T. Nguyen, R.S. Ruoff, Synthesis of graphene-based nanosheets via chemical reduction of exfoliated graphite oxide, Carbon 45 (2007) 1558–1565.

[47] S. Sun, Y. Cao, J. Feng, P. Wu, Click chemistry as a route for the immobilization of well-defined polystyrene onto graphene sheets, J. Mater. Chem. 20 (2010) 5605–5607.

[48] K.N. Kudin, B. Ozbas, H.C. Schniepp, R.K. Prud'homme, I.A. Aksay, R. Car, Raman spectra of graphite oxide and functionalized graphene sheets, Nano Lett. 8 (2008) 36–41.

[49] A.W. Coats, J.P. Redfern, Thermogravimetric analysis: a review, Analyst 88 (1963) 906–924.

[50] I. Jung, D. Dikin, S. Park, W. Cai, S.L. Mielke, R.S. Ruoff, Effect of water vapor on electrical properties of individual reduced graphene oxide sheets, J. Phys. Chem. C 112 (2008) 20264–20268.